

³¹F. Keffer, in *Handbuch der Physik*, edited by H. P. J. Wijn (Springer-Verlag, Berlin, 1966), Vol. XVIII/2, p. 123.

³²A. E. Meixner, R. E. Dietz, and D. L. Rousseau, *Bull. Am. Phys. Soc.* **17**, 335 (1972); and private communication.

³³P. Pincus, *Phys. Rev. Lett.* **5**, 13 (1960).

³⁴Two measurements of φ are reported in the literature: $\varphi=0.016$ rad (Ref. 8) and $\varphi=0.015$ rad (Ref. 4). We use the arithmetic mean.

PHYSICAL REVIEW B

VOLUME 7, NUMBER 11

1 JUNE 1973

Stress-Induced Spin Flop in Cr_2O_3 †

J. W. Allen

Lincoln Laboratory, Massachusetts Institute of Technology, Lexington, Massachusetts 02173

(Received 18 December 1972)

A complete phenomenological analysis of uniaxial stress-induced spin flop in Cr_2O_3 is given. The origins of the magnetic anisotropy and magnetoelastic interaction are discussed. The microscopic theory of the single-ion anisotropy and magnetoelastic interaction in ruby is reviewed, updated, and extended to Cr_2O_3 .

I. INTRODUCTION

Recently, in a paper¹ to be referred to hereafter as I, optical data were presented and interpreted as strong evidence that uniaxial stress induces spin flop in the uniaxial antiferromagnet Cr_2O_3 . The data consisted of the behavior of the ${}^4A_2 - {}^2E$ optical-exciton absorption spectrum when either a magnetic field was applied along the c axis or uniaxial stress was applied along the a axis of a sample of Cr_2O_3 . It was found that the changes induced in the spectrum as spin flop is forced by the applied magnetic field are nearly duplicated by the application of about 15 kbar of uniaxial stress. In a brief phenomenological discussion, based on a simple two-parameter magnetoelastic interaction, it was pointed out that very simple interrelations exist between the critical stresses required to induce spin flop and the magnetostrictive strains induced when spin flop is forced by a magnetic field. For Cr_2O_3 some of these strains have been measured by Dudko, Eremenko, and Semenenko² (DES). As pointed out in I, the interrelations predicted by the simple two-parameter magnetoelastic interaction discussed there are not satisfied by the data of DES and I. This discrepancy implies the need to consider the consequences of the most general magnetoelastic interaction allowed by crystal symmetry, and this is carried out in Sec. II of this paper. In I a brief discussion was also given of the origins of the magnetic anisotropy and magnetoelastic interaction in Cr_2O_3 . Section III extends that discussion, and Sec. IV discusses the microscopic theory of the single-ion anisotropy and magnetoelastic interaction.

II. PHENOMENOLOGICAL ANALYSIS OF CRITICAL STRESSES AND MAGNETOELASTIC STRAINS

In this section phenomenological expressions for the critical stresses required to produce spin flop

are obtained in terms of the elastic and magnetoelastic constants of the material. These expressions are then rewritten in terms of the magnetoelastic strains induced when spin flop is forced by an applied magnetic field, which provides the basis for a discussion of the relation of the results presented in I to the work of DES mentioned above. Such an analysis assumes small enough strains that magnetoelastic effects second order in the strains need not be considered and that Hook's law is obeyed. Although the analysis is straightforward, the portions dealing with stress-induced spin flop do not appear to have been given elsewhere before.³

In the absence of an applied stress, the magnetic anisotropy energy E_A can be written as $E_A = \sum_{ij} K_{ij} \alpha_i \alpha_j$, where K_{ij} is the anisotropy tensor and α_i is a direction cosine of the vector difference of the two sublattice magnetizations. The tensors K_{ij} and $\alpha_i \alpha_j$ are symmetric under interchange of i and j so it is convenient to employ the contracted indices notation of Voigt to write

$$E_A = \sum_j K_j \alpha_j. \quad (1)$$

The nonzero elements of K_j are restricted by the symmetry of the crystal. The presence of a strain ϵ_{ij} induces, through the magnetoelastic interaction, a further contribution to the anisotropy energy $\sum_{ijkl} \epsilon_{ij} F_{ijkl} \alpha_k \alpha_l$, as well as an elastic energy $\frac{1}{2} \sum_{ijkl} \epsilon_{ij} C_{ijkl} \epsilon_{kl}$, where F and C are the magnetoelastic and elastic tensors, respectively. These two energies may be written in Voigt's notation and added to (1) to give

$$E = \sum_j P_j \alpha_j + \frac{1}{2} \sum_{ij} \epsilon_i C_{ij} \epsilon_j, \quad (2)$$

where

$$P_j \equiv K_j + \sum_i \epsilon_i F_{ij}. \quad (3)$$

The nonzero elements of F_{ij} and C_{ij} are restricted

by the crystal symmetry. The equilibrium values of ϵ_i and α_j are those that simultaneously minimize the energy (2). However, it is convenient and realistic for the discussion of this paper to consider two simpler situations, first where the α_j are fixed and the ϵ_i can vary to minimize (2), and second where the ϵ_i are fixed and the α_j can vary to minimize (2).

For the first case where the α_j are fixed, the equilibrium ϵ_i , denoted by an overbar, are readily found as the solutions of the equations $\partial E/\partial \epsilon_i = 0$ to be

$$\bar{\epsilon}_i = - \sum_k \xi_{ik} \alpha_k, \quad (4)$$

where

$$\xi_{ik} \equiv \sum_j S_{ij} F_{jk} \quad (5)$$

and S_{ij} is the inverse of C_{ij} . Equation (4) can be used to find the magnetostrictive strains associated with spin flop or general spin rotation. It should be noted that Eq. (4) gives nonzero strains for the unflopped state; this is because, in the formulation being used, the unstrained state is the paramagnetic one. Thus the strains associated with spin rotation or spin flop are found by subtracting from the strains of the rotated state the strains of the unrotated state. By the simple artifice of replacing

$$F_{ij} \rightarrow [F_{ij} - F_{i3}(\delta_{j1} + \delta_{j2} + \delta_{j3})], \quad (6)$$

where it is assumed that the sublattice magnetizations lie along the z axis in the unrotated state, the unstrained state becomes the unrotated one, which is convenient for the discussion in this paper. It is readily verified that this change causes Eq. (4) to yield zero strains for the unrotated state and alters Eq. (2) only by subtracting a term $\sum_{j=1}^3 \sum_i \epsilon_i F_{i3} \alpha_j = \sum_i \epsilon_i F_{i3}$, which is independent of the α_j and hence leaves the magnetic anisotropy unchanged. This subtraction simplifies the induced-anisotropy tensor by making its Voigt-notation three-component zero, so it is convenient to make a similar subtraction from the quantity K_j and use for the energy

$$E = \sum_j Q_j \alpha_j + \frac{1}{2} \sum_{ij} \epsilon_i C_{ij} \epsilon_j, \quad (7)$$

where

$$Q_j \equiv P_j - K_3(\delta_{j1} + \delta_{j2} + \delta_{j3}) \quad (8)$$

and the altered F_{ij} of Eq. (6) are inserted in P_j . Q_j is then the total anisotropy in the presence of strains and has $Q_3 = 0$. Thus, the artifice provides a convenient zero reference for strains and excludes the isotropic part of the anisotropy tensor, which is irrelevant to the discussion at hand.

Finally, it should be noted that for a uniaxial crystal with the external magnetic field perfectly aligned with the c axis and spin flop occurring from

the c axis into the basal plane, the direction of the sublattice magnetizations in the basal plane is undetermined by the magnetic field or the uniaxial magnetic anisotropy. The direction will be fixed by the crystal distorting in the way that most lowers the energy (7). This situation requires that (7) be minimized simultaneously with respect to the ϵ_i and α_j and is hence outside the above discussion. In most experimental situations the external magnetic field is (intentionally or accidentally) slightly misaligned with the c axis, giving a small basal-plane component of field, which is assumed to be large enough to overcome the magnetoelastic energy and orient the sublattice magnetizations perpendicular to it. If this assumption is valid, then Eq. (4) will determine the strains when the spins are flopped.

In the second case the ϵ_i are assumed to be fixed through the application of an external stress T_k which causes strains $\epsilon_i = S_{ik} T_k$. Eliminating ϵ_i from (7) yields the energy in terms of T_k and the α_j as

$$E^k = \sum_j L_j^k \alpha_j + \frac{1}{2} T_k S_{kk} T_k, \quad (9)$$

where

$$L_j^k \equiv T_k \xi_{kj} + K_j - K_3(\delta_{j1} + \delta_{j2} + \delta_{j3}) \quad (10)$$

and the altered F_{ij} of Eq. (6) are used to find ξ_{kj} . The superscript k in (9) indicates that (9) is particular to a single component of applied stress being present. This is assumed here because both theory and experiment are simpler in this case. If more than one component of applied stress is present then the sum in the first term of (9) should also go over k and the second term is generalized to a form like the elastic energy part of (7). The α_k present in E^k must be consistent with the symmetry of the crystal in the presence of T_k , a requirement which is automatically met through the restrictions imposed by the unperturbed crystal symmetry on the matrices S_{ik} and F_{ij} . Spin reorientation will occur for a critical stress that causes the first term of (9), which will be denoted as E_{Ak} , to have an energy minimum for a different set of α_k than the set giving a minimum for $T_k = 0$. It is not convenient to set forth a general expression for this critical stress, since the details depend greatly on the particular situation. However, it can be noted that since both (4) and E_{Ak} involve only ξ_{ik} , the possibility exists for writing the critical stress in terms of some $\bar{\epsilon}_i$ and the K_j . For example, if spin flop occurs away from the z axis as the coefficient of α_x^2 is driven through zero by a z -axis stress, Eqs. (10) and (4) give for the critical stress $T_{\text{crit}} = (K_{xx} - K_{zz})/\bar{\epsilon}_{zz}(x)$, where $\bar{\epsilon}_{zz}(x)$ is the strain ϵ_{zz} when the magnetization is forced by a magnetic field to lie along the x axis. If the crystal is uniaxial and the z axis is the c axis, this

is also another example of a situation where (7) must be minimized simultaneously with respect to the ϵ_i and α_j . This is because the c -axis stress preserves the uniaxial form of the magnetic anisotropy so that the direction of the sublattice magnetizations in the basal plane after spin flop is undetermined. As in the discussion above for the case of spin flop induced by an external field lying exactly along the c axis, the basal-plane orientation will be determined by crystalline distortions, in this case, additional to the ones induced by the c -axis stress. This situation does not arise in the experiments discussed in this paper, because these experiments involve stress perpendicular to the c axis.

The application of the preceding results to Cr₂O₃ is fairly straightforward. Symmetry restrictions allow the following nonzero elements for the S , C , F , and K tensors in the Voigt notation⁴:

$$\begin{aligned}
 S_{ij}: & S_{11} = S_{22}, \quad S_{12}, \quad S_{13} = S_{23}, \quad S_{33}, \\
 & S_{14} = -S_{24} = \frac{1}{2}S_{56}, \quad S_{44} = S_{55}, \\
 & S_{66} = 2(S_{11} - S_{12}), \quad S_{ij} = S_{ji}; \\
 C_{ij}: & \text{same as for } S_{ij} \text{ except } C_{66} = \frac{1}{2}(C_{11} - C_{12}) \\
 & \text{and } C_{56} = C_{14}; \\
 F_{ij}: & F_{11} = F_{22}, \quad F_{12} = F_{21}, \quad F_{13} = F_{32}, \\
 & F_{14} = -F_{24} = F_{65}, \quad F_{41} = -F_{42} = F_{56}, \\
 & F_{33}, \quad F_{44} = F_{55}, \quad F_{66} = F_{11} - F_{12}; \\
 K_j: & K_1 = K_2, \quad K_3. \quad (11)
 \end{aligned}$$

The altered F_{ij} of Eq. (6) will be used and this entails the replacements $F_{11} - F_{11} - F_{13}$, $F_{31} - F_{31} - F_{33}$, $F_{12} - F_{12} - F_{13}$, $F_{13} - 0$, and $F_{33} - 0$. The quantity $K = K_1 - K_3$ will also appear. The forms of tensors given here are correct for the z axis lying along a C_3 axis, the crystal c axis, and the x axis lying along a C_2 axis, one of the three crystal a axes.

The effect of applied stresses T_1 , T_2 , and T_3 will be considered. In the presence of an arbitrary strain, the anisotropy tensor Q_j of Eq. (8) has triclinic symmetry with all elements unequal and nonzero. Thus in situations like the two mentioned above where the magnetic anisotropy is ultimately

determined by spontaneous crystalline distortions, it is possible for the crystal to distort so that Q_j loses all symmetry if it is energetically advantageous for this to occur. If the strains ϵ_i are nonzero only for $i = 1, \dots, 4$, Q_j has monoclinic symmetry with nonzero unequal elements for $j = 1, 2, 4$, and since the crystal has monoclinic symmetry in the presence of applied stress along or perpendicular to an a axis, that is T_1 or T_2 , it is not surprising to find that the above combination of strains is induced by either T_1 or T_2 and that the anisotropy tensor L_j^k of Eq. (10) has monoclinic symmetry with unequal nonzero elements for $j = 1, 2, 4$ and $k = 1, 2$. Similarly, an applied stress T_3 leaves the crystal trigonal, induces strains $\epsilon_1 = \epsilon_2, \epsilon_3$, and gives an L_j^k with trigonal symmetry and nonzero elements $L_1^3 = L_2^3$.

Further simplification may be achieved only by adopting a less general magnetoelastic interaction as done, for example, by DES,² who set $F_{11} = F_{12}$ and $F_{14} = F_{41} = F_{44} = 0$ (altered F_{ij}). From Eq. (4) it is readily seen that these conditions ensure that trigonal symmetry is maintained for arbitrary α_k by permitting only the strains $\bar{\epsilon}_1 = \bar{\epsilon}_2$ and $\bar{\epsilon}_3$. This is a two-parameter magnetoelastic interaction obtained by expanding K in these strains. DES have chosen to expand in terms of ϵ_3 and $(\epsilon_1 + \epsilon_2 + \epsilon_3)$ with coefficients λ_1 and λ_2 , respectively. It is straightforward to identify $\lambda_1 = F_{31} + F_{13} - F_{33} - F_{11}$ and $\lambda_2 = F_{11} - F_{13}$, using the original, unaltered F_{ij} . Such an interaction leads to a trigonal L_j^k for arbitrary k .

The next step is to find the various possible energy minima of $E_{Ak} = \sum_j L_j^k \alpha_j$ as the α_j are varied. For this it is convenient to relabel the L_j^k more simply by $L_1^k = a$, $L_2^k = b$, $L_4^k = d$ for all k . Of course the actual expressions for a , b , and d depend upon k . Using spherical coordinates with polar axis along z and ϕ the polar angle to specify the α_j gives the following form to be minimized:

$$\mathcal{E}_A = a \sin^2 \phi \cos^2 \theta + b \sin^2 \phi \sin^2 \theta + 2d \sin \phi \cos \phi \sin \theta. \quad (12)$$

Standard techniques then show energy minima for the following possible combinations of a , b , d and directions of the vector difference of the two sublattice magnetizations, denoted by \vec{L} (note that \vec{L} and $-\vec{L}$ are physically equivalent):

- (i) $d = 0$, $a = b > 0$ (trigonal symmetry); $\phi = 0$; $\mathcal{E}_{A \min} = 0$; \vec{L} points along z ;
- (ii) $d = 0$, $a = b < 0$ (trigonal symmetry); $\phi = \frac{1}{2}\pi$; θ undetermined; $\mathcal{E}_{A \min} = a$;
 \vec{L} lies in the x - y plane;
- (iii) $d = 0$, $a \neq b$, $a, b > 0$; $\phi = 0$; $\mathcal{E}_{A \min} = 0$; \vec{L} points along z ;
- (iv) $d = 0$, $a < 0$, and $a < b$; $\phi = \frac{1}{2}\pi$; $\theta = 0$; $\mathcal{E}_{A \min} = a$; \vec{L} lies along x ;
- (v) $d = 0$, $b < 0$, and $b < a$; $\phi = \frac{1}{2}\pi$; $\theta = \frac{1}{2}\pi$; $\mathcal{E}_{A \min} = b$; \vec{L} lies along y ;

- (vi) $d > 0$, $a = b = 0$; $\phi = \frac{1}{4}\pi$; $\theta = \frac{1}{2}\pi$; $\mathcal{E}_{A \min} = -d$; \vec{L} lies in the y - z plane;
- (vii) $d < 0$, $a = b = 0$; $\phi = \frac{3}{4}\pi$; $\theta = \frac{1}{2}\pi$; $\mathcal{E}_{A \min} = -d$; \vec{L} lies in the y - z plane;
- (viii) $d \neq 0$, b arbitrary; $\tan 2\phi = -2d/b$, with $0 \leq 2\phi \leq \pi$ for $d < 0$ and $\pi \leq 2\phi \leq 2\pi$ for $d > 0$, $\theta = \frac{1}{2}\pi$; $\mathcal{E}_{A \min} = \frac{1}{2}[b - (b^2 + 4d^2)^{1/2}]$;
 \vec{L} lies in the y - z plane;
- (ix) $a < \frac{1}{2}[b - (b^2 + 4d^2)^{1/2}]$, b and d arbitrary; $\phi = \frac{1}{2}\pi$, $\theta = 0$; $\mathcal{E}_{A \min} = a < 0$;
 \vec{L} lies along x ;
- (x) $a(a - b) = d^2$; $\tan \phi = \frac{a/d}{\sin \theta}$; $\mathcal{E}_{A \min} = a = \frac{1}{2}[b - (b^2 + 4d^2)^{1/2}]$;

direction of \vec{L} undetermined in a plane containing \vec{L} 's directions in cases (viii) and (ix).

Using Eqs. (6), (10), and (11), expressions for a , b , and d in the instances of applied stresses T_1 , T_2 , and T_3 can be found as follows:

$$\begin{aligned} T_1: & a = K + \alpha T_1, \quad b = K + \beta T_1, \quad d = \delta T_1; \\ T_2: & a = K + \beta T_2, \quad b = K + \alpha T_2, \quad d = -\delta T_2; \\ T_3: & a = K + \gamma T_3, \quad b = K + \gamma T_3, \quad d = 0, \end{aligned} \quad (13)$$

where α , β , δ , and γ are given in terms of unaltered F_{ij} and S_{ij} by the formulas

$$\begin{aligned} \alpha &= [S_{11}(F_{11} - F_{13}) + S_{12}(F_{12} - F_{13}) \\ &\quad + S_{13}(F_{31} - F_{33}) + S_{14}F_{41}], \\ \beta &= [S_{11}(F_{12} - F_{13}) + S_{12}(F_{11} - F_{13}) \\ &\quad + S_{13}(F_{31} - F_{33}) - S_{14}F_{41}], \\ \delta &= [S_{11}F_{14} - S_{12}F_{14} + S_{14}F_{44}], \\ \gamma &= [S_{13}(F_{11} - F_{13}) + S_{13}(F_{12} - F_{13}) + S_{33}(F_{31} - F_{33})]. \end{aligned} \quad (14)$$

Using Eqs. (4) and (5), α , β , δ , and γ can also be expressed in terms of equilibrium strains for certain directions of \vec{L} as follows:

$$\begin{aligned} \alpha &= -[\bar{\epsilon}(x) + \bar{\Delta}(x)], \\ \beta &= -[\bar{\epsilon}(x) - \bar{\Delta}(x)], \\ \delta &= -\frac{2}{3}\bar{\Delta}(xyz), \\ \gamma &= -\bar{\epsilon}_{zz}(x), \end{aligned} \quad (15)$$

where $\bar{\epsilon}$ and $\bar{\Delta}$ are defined by the relations

$$\begin{aligned} \bar{\epsilon}_{xx}(l) &\equiv [\bar{\epsilon}(l) + \bar{\Delta}(l)], \\ \bar{\epsilon}_{yy}(l) &\equiv [\bar{\epsilon}(l) - \bar{\Delta}(l)], \end{aligned} \quad (16)$$

and the notation $\bar{f}(l)$ means, for $l = x$, y , and xyz , respectively, that \bar{f} is evaluated for $\alpha_j = \delta_{j1}$, δ_{j2} , and $\frac{1}{3}$. The double-subscript notation for the strains has been reintroduced for physical clarity. For later use it can also be noted that the equilibrium strains satisfy the following interrelations:

$$\bar{\epsilon}_{xx}(x) = \bar{\epsilon}_{yy}(y),$$

$$\begin{aligned} \bar{\epsilon}_{yy}(x) &= \bar{\epsilon}_{xx}(y), \\ \bar{\epsilon}_{zz}(x) &= \bar{\epsilon}_{zz}(y), \\ \bar{\epsilon}(x) &= \bar{\epsilon}(y), \\ \bar{\Delta}(x) &= -\bar{\Delta}(y). \end{aligned} \quad (17)$$

The variation in the direction of \vec{L} with stress shows a remarkably wide range of quite appealing possibilities, depending on the values of K , α , β , δ , and γ . For T_1 stress, this is illustrated by the sketches of Fig. 1, which assume a positive K , as is appropriate for Cr_2O_3 . For no applied stress, positive K corresponds to energy minimum case (i) above, and \vec{L} lies initially along the z (trigonal) axis. The results shown in Fig. 1 are obtained by systematically examining the consequences of substituting the T_1 expressions for a , b , and d from Eqs. (13) into the energy minima results summarized above. There are basically four types of behavior, which occur in various combinations. The four types can be seen in the Fig. 1 sketches for negative (compressive) T_1 . For $\alpha^- < \alpha < \alpha^+$, where

$$\begin{aligned} \alpha^+ &\equiv \frac{1}{2}[\beta + (\beta^2 + 4\delta^2)^{1/2}], \\ \alpha^- &\equiv \frac{1}{2}[\beta - (\beta^2 + 4\delta^2)^{1/2}], \end{aligned} \quad (18)$$

the motion of \vec{L} is always in the y - z plane ($\theta = \frac{1}{2}\pi$). The actual value of ϕ is determined by the equation

$$\tan 2\phi = -\frac{2(\delta/\beta)T_1}{(K/\beta) + T_1}, \quad (19)$$

where for $T_1 > 0$ ($T_1 < 0$), ϕ is between 0 and $\frac{1}{2}\pi$ if $\delta < 0$ ($\delta > 0$) and between $\frac{1}{2}\pi$ and π if $\delta > 0$ ($\delta < 0$). There are two possibilities, depending on the sign of β . Considering for the moment negative T_1 only, if $\beta < 0$, ϕ is restricted to the region between 0 and $\frac{1}{4}\pi$ or between π and $\frac{3}{4}\pi$, depending on the sign of δ . Note that \vec{L} and $-\vec{L}$ are physically equivalent, so that the configurations $\phi = 0$ and $\phi = \pi$ are equivalent, as are configurations for $\theta = \frac{1}{2}\pi$, ϕ and $\theta = \frac{3}{2}\pi$, $\pi - \phi$. For $\beta > 0$, the denominator of Eq. (19) is

driven through 0 at $T_1 = -K/\beta$ so that \vec{L} rotates to a position where ϕ is between $\frac{1}{4}\pi$ and $\frac{1}{2}\pi$, or between $\frac{3}{4}\pi$ and $\frac{1}{2}\pi$, again depending on the sign of δ . If $|\delta/\beta| \ll 1$, \vec{L} will tend to flip abruptly from the z to the y axis. Large values of $|\delta/\beta|$ tend to broaden out the region of fast change and draw the final equilibrium position away from the y axis to a point midway between the y and z axes. The two cases just discussed both correspond to energy minimum case (viii) above.

Still considering only negative T_1 , if $\alpha > \alpha^+$, the motion of \vec{L} in either of the two cases just discussed is interrupted by an abrupt flip to the x axis at a stress and angle given by

$$T_{1c} = -K(\alpha - \beta) / [\alpha(\alpha - \beta) - \delta^2], \quad (20)$$

$$\tan\phi_c = \delta / (\alpha - \beta). \quad (21)$$

This additional possibility, which corresponds to energy minima case (ix) above, increases the possibilities to four, as mentioned previously. Evidently, for positive T_1 the first two cases [involving Eq. (19)] can occur with reversed signs of δ and β , and it is found that the second two cases [involving Eq. (20)] occur for $\alpha < \alpha^-$. Combinations of these possibilities produce the entire picture presented in Fig. 1. The two conditions for T_{1c} to be relevant, $\alpha > \alpha^+$ or $\alpha < \alpha^-$, are the conditions that $\alpha(\alpha - \beta) > \delta^2$, which is required to make energy minima case (ix) more stable than case (viii). Thus the denominator of Eq. (20) is always positive. Note that α^+ is always greater than 0 or β , and that α^-

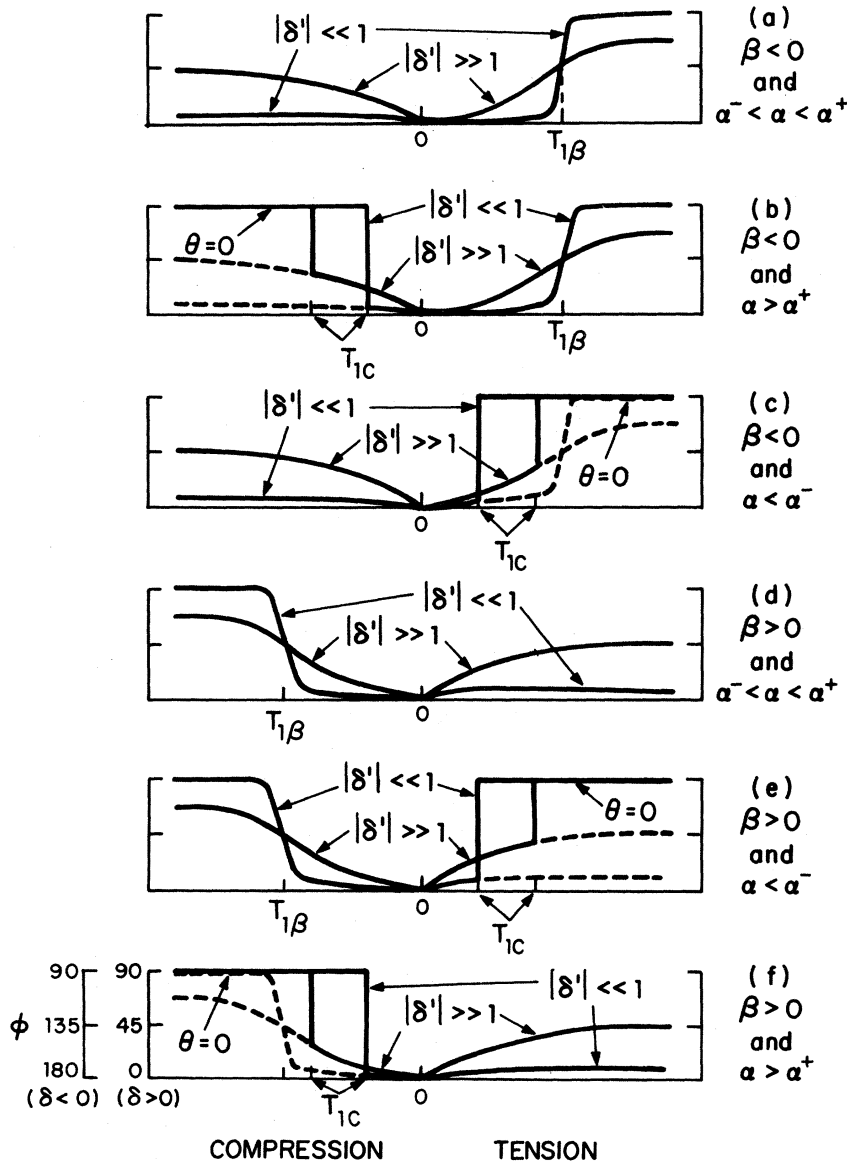


FIG. 1. Possible variations in the direction of the antiferromagnetism vector \vec{L} for T_{xx} applied stress. The various parameters appearing in the figure are defined in the text. Motion is in the y - z plane, $\theta = \frac{1}{2}\pi$, except for flips to the x axis, denoted by $\theta = 0$. The dotted lines show the variation of \vec{L} 's direction if the motion were not interrupted by a flip to the x axis.

is always less than 0 or β , which leads to the correlation between α^+ and $T_{1c} < 0$, and between α^- and $T_{1c} > 0$. It is interesting to consider the relations between $T_{1\beta}$ and T_{1c} and the effect of α and δ upon this relation. $T_{1c}/T_{1\beta}$ has the same sign as $\alpha/\beta \equiv \alpha'$. Figure 2 shows, in the $\alpha' - |\delta'|$ plane (where $\delta' \equiv \delta/\beta$), lines where $T_{1c}/T_{1\beta}$ equals ± 1 and $\pm \infty$. The $+1$ line is $\alpha' = 1 + |\delta'|$, and the -1 line is $-(1 + \delta'^2)^{1/2}$. The $\pm \infty$ lines are essentially plots of α^+/β and α^-/β . It can be seen that the regions where $1 < |T_{1c}/T_{1\beta}| < \infty$ are very narrow and that increasing $|\delta'|$ for fixed α and β increases $|T_{1c}/T_{1\beta}|$.

The possible behaviors for stress T_2 (perpendicular to an a axis) can readily be deduced, according to Eq. (13), from the results just presented by the replacements $\alpha \rightarrow \beta$, $\beta \rightarrow \alpha$, and $\delta \rightarrow -\delta$. Thus the behavior of the direction of \vec{L} associated with

$T_{1\beta}$ and T_{1c} will occur for critical values of T_2 given by, respectively,

$$\begin{aligned} T_{2\alpha} &= -\frac{K}{\alpha}, \\ T_{2c} &= -\frac{K(\beta - \alpha)}{\beta(\beta - \alpha) - \delta^2}, \end{aligned} \quad (22)$$

and with T_{2c} there will be associated appropriate β^* and β' values. These, and the preceding results, lead to the statement made in I that combinations of parameters are possible such that "compressive (tensile) stress along or perpendicular to an a axis induces the spins to flop into the basal plane perpendicular to (along) or along (perpendicular to) the a axis, respectively." The behavior for stress T_3 is much simpler. At $T_{3y} = -K/\gamma$, the spins flop from the z axis into the basal plane, the direction in the basal plane being undetermined by this analysis as discussed above.

Less general magnetoelastic interactions yield simpler behavior than that just described. For example, Eq. (14) shows that if $F_{14} = F_{41} = F_{44} = 0$, then $\delta = 0$ but α need not equal β . For $\delta = 0$, all the spin flops become sharp from the z axis to the x or y axes. In addition, $T_{1c} = T_{1\alpha} \equiv -K/\alpha$, and α^+ and α^- are either β or 0 depending on the sign of β . These changes result in the simplified diagrams of Fig. 3. The energy minima involved are cases (iii)-(v). As already mentioned, the even less general magnetoelastic interaction adopted by DES² predicts for an arbitrary direction of \vec{L} that $\bar{\epsilon}_{xx} = \bar{\epsilon}_{yy}$ and that only these strains and $\bar{\epsilon}_{zz}$ ever occur. Thus, from Eq. (16), $\bar{\Delta}$ is always zero, so Eq. (15) shows that

$$\begin{aligned} \alpha &= \beta = -\bar{\epsilon}(x), \\ \delta &= 0, \\ \gamma &= -\bar{\epsilon}_{zz}(x). \end{aligned} \quad (23)$$

Thus, for this model, there is only one critical basal-plane stress $T_{1\alpha} = T_{1\beta} = -K/\alpha$, and the spin flop is sharp from the z axis into the basal plane with the basal-plane direction undetermined. The two possible behaviors for stress T_1 are like those of Figs. 3(a) and 3(d). The energy minima involved are cases (i) and (ii). The only special energy minima cases not discussed here are (vi), (vii), and (x) because they do not appear to be at all relevant to the behavior of Cr_2O_3 .

As mentioned at the outset of this paper, the behavior of the optical spectrum of Cr_2O_3 with the crystal subjected to T_1 stress of about -15 kbar is very similar to the behavior of the spectrum when spin flop is forced by application of a c -axis magnetic field. This leads to the presumption that the stress is inducing spin flop essentially from the z axis into the basal plane. That the flop appears to occur from ϕ near 0 to ϕ near $\frac{1}{2}\pi$ strongly suggests

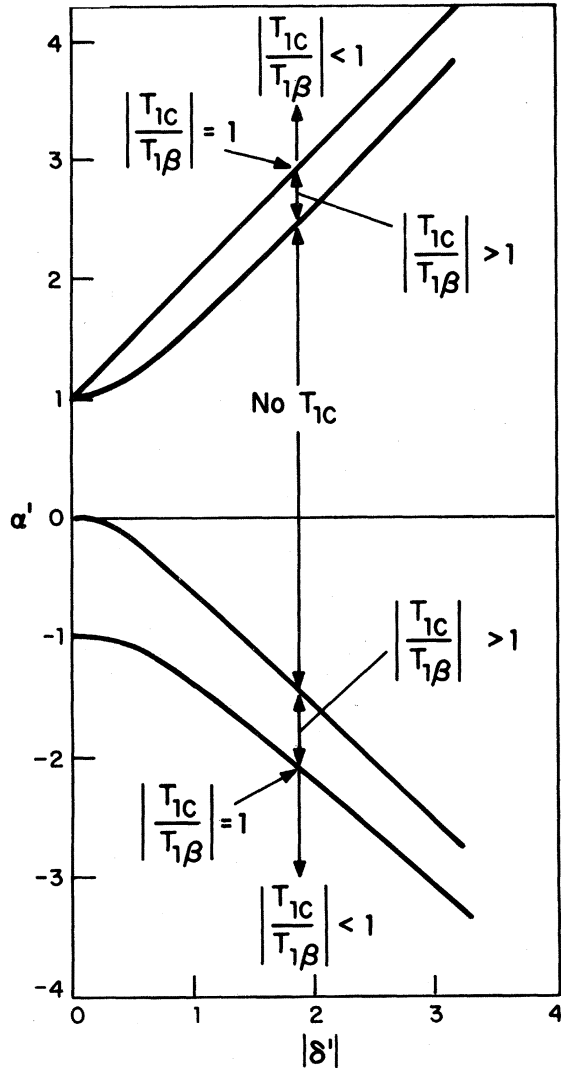


FIG. 2. Variation of $\alpha' = \alpha/\beta$, with $|\delta| = |\delta/\beta|$, parametrized in $|T_{1c}/T_{1\beta}|$.

that $|\delta'|$ cannot be very large, since one effect of a nonzero δ is to reduce that range of ϕ over which the transition occurs, as shown in Fig. 1. Some experimentation with Eq. (19) indicates that $|\delta'| < 0.1$ would be consistent with the data. A second consequence of nonzero δ is the spreading of the region of T_1 over which a rapid change in ϕ takes place for the transition involving $T_{1\beta}$. While the changes observed in the optical spectrum were fairly abrupt, they were not, in fact, sharp. In I it was argued that this was probably due to inhomogeneities in the stress applied to the sample during the experiment. The stress was observed to broaden the lines by about 5 cm^{-1} and from the linear shifts observed in the line positions at low stress, it can be inferred that there was a stress distribution of about 4 kbar, which is about the

width of the region of rapid change in the spectrum. However, the total range of T_1 over which there occur departures from the low-stress linear shift of line positions is about $-20 < T_1 < -11$, rather larger than 4 kbar. This suggests that δ is not zero and the upper limit $|\delta'| < 0.1$ argued for above is consistent with the observed spreading, assuming that the transition involves $T_{1\beta}$ and that the variation of the line positions with ϕ is reasonably smooth. It is very difficult to separate this effect from that involving stress inhomogeneities, and it is likely that both are present.

From the experimental data, and taking account of the difficulties just mentioned, it is not presently possible to distinguish conclusively among the various possibilities shown in Fig. 1, except to eliminate Figs. 1(a) and 1(c), where no transition occurs for compressive stress, and to argue that $|\delta'|$ is small. There are, then, two possibilities, either that $T_{1\beta} \cong -15 \text{ kbar}$ or that $T_{1\alpha} \cong -15 \text{ kbar}$. For the first case, using the value $K = 2 \times 10^5 \text{ ergs/cm}^3$ determined from antiferromagnetic resonance and the formula for $T_{1\beta}$, it is readily determined that $\beta \cong 1.33 \times 10^{-5}$. To discuss the second case, it is convenient to rewrite Eq. (20) as

$$T_{1c} = -\frac{K}{\alpha} \left(\frac{1}{1 - \delta'^2/\alpha'(\alpha' - 1)} \right), \quad (24)$$

from which it can be seen that for $|\delta'| < 0.1$, and assuming, as will be discussed further below, that $|\alpha'| > 2.0$, then $T_{1c} \cong -K/\alpha$. This approximation leads to $\alpha \cong 1.33 \times 10^{-5}$.

It is now appropriate to discuss the work of DES^{2,5} in relation to the work presented here. In one experiment,⁵ they measured the change in critical magnetic field for spin flop (H_c) due to compressive stress T_3 . They found a linear increase in H_c for $|T_3|$ up to 2.5 kbar. If these data are extrapolated linearly to positive T_3 , it is found that H_c is driven to zero at about +7 kbar, implying that $T_{3\gamma} = +7 \text{ kbar}$, and that $\gamma = -2.86 \times 10^{-5}$. In a second experiment, DES measured the strains induced along the c axis and in the basal plane when spin flop is forced by a magnetic field. They found $\bar{\epsilon}_{zz} = +2.8 \times 10^{-5}$. These experimental results for γ and $\bar{\epsilon}_{zz}$ are in excellent agreement with the expression for γ in Eqs. (15) and (23), which invites confidence in the assumptions made at the outset of the phenomenological analysis. The basal-plane strain measurements require some interpretation. They were made along an axis, to be denoted as x' , lying in the basal plane at an unspecified angle θ to a crystal a axis. The applied magnetic field was tilted slightly from the c axis, producing a basal-plane component H_1 that was assumed to orient the spins in the basal plane after spin flop occurred. Strain measurements were made along x' for H_1 oriented along and perpendicular to x' . It is straightforward

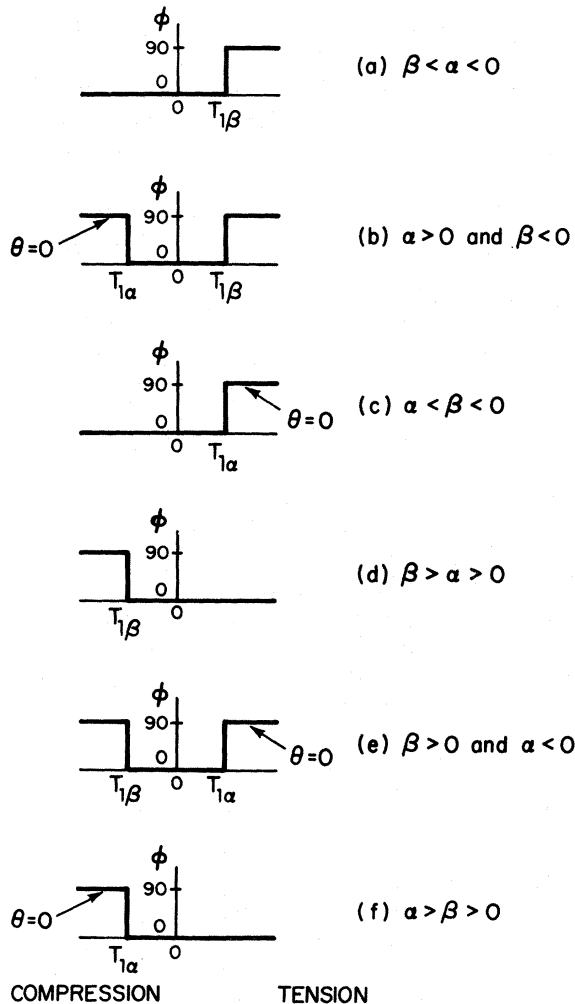


FIG. 3. Possible variations in the direction of \vec{L} for the simplified magnetoelastic interactions giving $\delta = 0$.

to rotate the strain tensor by an angle θ in the basal plane to obtain $\bar{\epsilon}_{x'x'}$ in terms of $\bar{\epsilon}_{xx}$, $\bar{\epsilon}_{yy}$, $\bar{\epsilon}_{xy}$, and θ . Assuming that H_1 oriented the spins parallel and perpendicular to x' , Eq. (4) can be used to find $\bar{\epsilon}_{xx}$, $\bar{\epsilon}_{yy}$, and $\bar{\epsilon}_{xy}$ in terms of S_{ij} , F_{jk} , and θ for the two experiments. When these are substituted in the expression for $\bar{\epsilon}_{x'x'}$, the result is, fortunately, independent of θ . For \bar{L} along x' , $\bar{\epsilon}_{x'x'}(\parallel) = \bar{\epsilon}_{xx}(x)$ and for \bar{L} perpendicular to x' , $\bar{\epsilon}_{x'x'}(\perp) = \bar{\epsilon}_{xx}(y)$. From Eq. (17), the latter quantity is also equal to $\bar{\epsilon}_{yy}(x)$, so the measurements of DES yield the strains appearing in Eq. (16). DES report only the average value of their two basal-plane strain measurements, this being the quantity $\bar{\epsilon}(x)$ appearing in Eqs. (15) and (16), and they find $\bar{\epsilon}(x) = -0.4 \times 10^{-5}$.

DES introduce the simplified two-parameter magnetoelastic interaction that has been described above to analyze their results.² Using the restrictions imposed by this model on the F_{ij} , Eqs. (4) and (5) can be used to find the following results, obtained by DES and expressed in terms of their parameters λ_1 and λ_2 , defined above:

$$\begin{aligned}\bar{\epsilon}_{xx} = \bar{\epsilon}_{yy} &= -(\alpha_1 + \alpha_2) \{ \lambda_1 S_{13} + \lambda_2 (S_{11} + S_{12} + S_{13}) \}, \\ \bar{\epsilon}_{zz} &= -(\alpha_1 + \alpha_2) \{ \lambda_1 S_{33} + \lambda_2 (2S_{13} + S_{33}) \}, \\ 2\bar{\epsilon}(x) + \bar{\epsilon}_{zz} &= -(\alpha_1 + \alpha_2) \{ \lambda_1 (2S_{13} + S_{33}) + \lambda_2 (2S_{11} \\ &\quad + 2S_{12} + 4S_{13}) \}.\end{aligned}\quad (25)$$

The latter two of these equations can be inverted to find λ_1 and λ_2 in terms of $\bar{\epsilon}(x)$, $\bar{\epsilon}_{zz}(x)$, and the various S_{ij} . Using the results of hydrostatic stress-

TABLE I. Values of parameters defined in text that follow from each of the two possible interpretations of the observed critical stress for spin flop.

$T_{1\beta} = -15$ kbar	$T_{1c} = -15$ kbar
$\beta = -\bar{\epsilon}_{yy}(x) = 1.33 \times 10^{-5}$	$\alpha = -\bar{\epsilon}_{xx}(x) = 1.33 \times 10^{-5}$
$\alpha = -\bar{\epsilon}_{xx}(x) = -0.53 \times 10^{-5}$	$\beta = -\bar{\epsilon}_{yy}(x) = -0.53 \times 10^{-5}$
$\bar{\Delta}(x) = +0.93 \times 10^{-5}$	$\bar{\Delta}(x) = -0.93 \times 10^{-5}$
$ \delta' < 0.1$	$ \delta' < 0.1$
$ \delta < 1.33 \times 10^{-6}$	$ \delta < 0.53 \times 10^{-6}$
$T_{1c} = 38.5$ kbar	$T_{1\beta} = 37.8$ kbar
$\alpha^* = 1.344 \times 10^{-5}$	$\alpha^* = 0.005 \times 10^{-5}$
$\alpha^- = -0.014 \times 10^{-5}$	$\alpha^- = -0.535 \times 10^{-5}$
$\alpha' = -0.398$	$\alpha' = 2.51$
Fig. 1(e)	Fig. 1(b)
$T_{2\alpha} = +37.8$ kbar	$T_{2\alpha} = -15$ kbar
$T_{2c} = -15.15$ kbar	$T_{2c} = +38.5$ kbar
$\beta^* = 0.005 \times 10^{-5}$	$\beta^* = 1.344 \times 10^{-5}$
$\beta^- = -0.535 \times 10^{-5}$	$\beta^- = -0.014 \times 10^{-5}$

TABLE II. Experimental and theoretical values are for various Cr_2O_3 static magnetoelastic constants F_{ij} . The experimental values are for the case $T_{1c} = -15$ kbar of Table I.

	Experimental (10^7 erg/cm ³)	Magnetic dipole (10^7 erg/cm ³)	Single ion (10^7 erg/cm ³)
$F_{11} + F_{12} - 2F_{13}$	-0.8	-0.94	9.78
$F_{31} - F_{33}$	-24.4	1.31	-11.91
$F_{11} - F_{12}$			8.08
F_{41}			-0.53
F_{14}			-0.78
F_{44}			2.44
$(F_{11} - F_{12}) + 0.22F_{41}$	4.36		7.96
$F_{44} + 4.54F_{14}$	mag. < 0.56		-1.20
$(F_{11} - F_{13}) + 0.11F_{41}$	1.78		8.88
$(F_{12} - F_{13}) - 0.11F_{41}$	-2.58		0.91

strain measurements for Cr_2O_3 ,⁶ and the Al_2O_3 value⁷ of $\mu \equiv -S_{13}/S_{33}$, which is not known for Cr_2O_3 , DES find the two λ values to be $\lambda_1 = -24 \times 10^7$ ergs/cm³ and $\lambda_2 = -0.4 \times 10^7$ ergs/cm³. For the magnetoelastic interaction of DES, α and β are both, from Eq. (23), equal to $-\bar{\epsilon}(x) = +0.4 \times 10^{-5}$, which compares very badly with the possible values of α and β (1.33×10^{-5}) determined in the experiments reported here. Indeed, the critical stress for spin flop would be $-K/\alpha = -50$ kbar, a value so large that it would surely preclude observation of the effect.

Unless a large error is assumed to exist either in the strain measurements of DES or the present stress measurements, this discrepancy implies the need to consider a less restrictive magnetoelastic interaction, as has been done in the earlier parts of this paper. The more general results for α and β , given in Eq. (15), do indeed evade the conflict between the measured values of critical stress and $\bar{\epsilon}(x)$ by allowing $\bar{\Delta}(x)$ to be nonzero so that α and β need not be equal to $-\bar{\epsilon}(x)$ or to each other. As previously discussed there are two interpretations of the observed critical stress, one yielding a value for α and the other a value for β . Using the experimental $\bar{\epsilon}(x)$ of DES, and the following results, obtained from Eqs. (15),

$$\alpha + \beta = -2\bar{\epsilon}(x), \quad (26)$$

$$\bar{\Delta}(x) = \frac{1}{2}(\beta - \alpha),$$

the unknown quantity, α or β , as well as $\bar{\Delta}(x)$, can be obtained for each possibility. These results are summarized in Table I, along with various other quantities of interest that can be computed. Where $|\delta'|$ has been needed, it has been set to 0.1. For both cases, α has a value, relative to α^+ or α^- , that allows a T_{1c} to exist. For the case $T_{1c} = -15$ kbar, the assumption made originally in obtaining a value for α , that $|\alpha'| > 2.0$, is well satisfied. Once values of α , β , and δ are found, it is

possible to determine uniquely which diagram of Fig. 1 is pertinent, and this is given in Table I. The critical T_2 stresses are readily found in accordance with Eqs. (22) and the associated discussion. They are also given in Table I, and show that a compressive stress of about -15 kbar applied perpendicular to an a axis should also induce spin flop. This result has not been verified experimentally. One disturbing aspect of the results of Table I should be pointed out. This is that $\bar{\epsilon}_{yy}(x)$ and $\bar{\epsilon}_{xx}(y)$ have opposite signs, and while DES imply that these quantities are not experimentally equal, it might be supposed that if they had opposite signs, this would have been mentioned by DES.

The final effort that can be made is to try to deduce the various (unaltered) F_{ij} , assuming all the pieces of experimental data are correct. The data of DES are related to the F_{ij} through the latter two of Eqs. (25) with λ_1 and λ_2 replaced, respectively, by the more general quantities λ'_1 and λ'_2 , which are defined by

$$\begin{aligned}\lambda'_1 &= F_{31} + F_{13} - F_{33} - \frac{1}{2}(F_{11} + F_{12}), \\ \lambda'_2 &= \frac{1}{2}(F_{11} + F_{12}) - F_{13}.\end{aligned}\quad (27)$$

The restrictions on F_{ij} imposed by the model of DES cause the two primed quantities to reduce to the unprimed ones. Since the form of Eqs. (25) is unaltered, the results of DES for $\lambda_{1,2}$ may be taken over for $\lambda'_{1,2}$. Thus the data of DES yield the linear combinations of F_{ij} given in the first two rows of the first column of Table II. The stress experiments of this paper yield $\bar{\Delta}(x)$ and an upper limit for $|\delta|$. Using Eqs. (26) and (14), $\bar{\Delta}(x)$ is related to the F_{ij} by

$$\bar{\Delta}(x) = -S_{14}F_{41} - \frac{1}{2}(F_{11} - F_{12})(S_{11} - S_{12}), \quad (28)$$

and Eq. (14) gives the equivalent expression for δ . Using either of these two expressions requires knowing S_{14} and $(S_{11} - S_{12})$, which have not been measured for Cr_2O_3 . To find approximate values for the unknown S_{ij} , the procedure of DES, mentioned below Eq. (25), has been adopted. Hydrostatic stress-strain measurements⁶ have given the following linear combinations of S_{ij} :

$$\begin{aligned}S_{33} + 2S_{13} &= 0.077 \times 10^{-12} \text{ cm}^2/\text{dyn}, \\ S_{33} + 2S_{11} + 2S_{14} + 4S_{13} &= 0.5 \times 10^{-12} \text{ cm}^2/\text{dyn}.\end{aligned}\quad (29)$$

With the assumption that $\mu = -S_{13}/S_{33}$ and $\nu = -S_{12}/S_{11}$ have the same values as in Al_2O_3 , 0.174 and 0.297, respectively,⁷ approximate values for the S_{ij} can be obtained as

$$\begin{aligned}S_{33} &= 0.118 \times 10^{-12}, \quad S_{13} = -0.02 \times 10^{-12}, \\ S_{11} &= 0.329 \times 10^{-12}, \quad S_{12} = -0.098 \times 10^{-12}.\end{aligned}$$

For S_{14} there is little recourse but to use the Al_2O_3 value⁷ of $S_{14} = 0.047 \times 10^{-12}$. The units of all the S_{ij}

are cm^2/dyn . This procedure then leads to the following results for linear combinations of the F_{ij} , where the upper number or sign is for the case $T_{1b} = -15$ kbar:

$$\begin{aligned}(F_{11} - F_{12}) + 0.22 F_{41} &= \mp 4.36 \times 10^7 \text{ erg/cm}^3, \\ F_{44} + 4.54 F_{14} &= \begin{cases} 1.42 \times 10^7 \\ 0.565 \times 10^7 \end{cases} \text{ erg/cm}^3.\end{aligned}\quad (30)$$

The values for the case $T_{1c} = -15$ kbar (lower number and sign) are given in the first column of Table II for later comparison with theory, as these values come closest to the theoretical ones. The last two rows of Table II can be deduced from the first and seventh rows. This is as far as the determination of the F_{ij} can be carried at present and even these results should not be viewed with much reverence due to the uncertainties in the data and the S_{ij} . They are presented here mainly to indicate the probable magnitudes of the various F_{ij} . Distinguishing between the two cases of Table I will probably entail further experimental information as will the determination of the actual F_{ij} values for Cr_2O_3 .

III. ORIGINS OF THE MAGNETIC ANISOTROPY AND MAGNETOELASTIC INTERACTION IN Cr_2O_3

The magnetoelastic interaction is basically the strain dependence of the anisotropy energy, and the anisotropy energy has contributions from the single-ion crystalline field anisotropy, the magnetic dipole-dipole interior interaction, and the anisotropy of the interior exchange interaction (pseudodipolar interaction). The contributions of these three mechanisms to the anisotropy constant K of Cr_2O_3 have been assessed by Artman, Murphy, and Foner.⁸ They presume that the exchange anisotropy is negligibly small. They calculate the dipole-dipole contribution, K_{MD} , to be 10^5 erg/cm^3 , and subtract this number from the experimental value of K , determined by antiferromagnetic resonance to be $2 \times 10^5 \text{ erg/cm}^3$, to obtain the single-ion contribution, K_S , as 10^5 erg/cm^3 .

The assumption that the exchange anisotropy, K_E , is negligible may not be justified for Cr_2O_3 . Taking as unperturbed basis states the Cr^{3+} states in the cubic approximation with no spin-orbit coupling, the order of magnitude of K_E and K_S can be estimated as $K_E \sim (\xi/\Delta E)^2 J'$ and $K_S \sim (\xi/\Delta E)^2 (v, v')$, where ξ is the spin-orbit parameter, ΔE is the separation of the ground and excited states, J' is an excited-state exchange interaction, and v, v' are the trigonal crystal-field parameters. Arguments will be presented below that J' and (v, v') may be comparable in Cr_2O_3 so that K_E is not a priori negligible compared to K_S . For the moment, then, the conclusions of Artman, Murphy, and Foner are modified here to state that $(K_E + K_S) = 10^5 \text{ erg/cm}^3$. An important point regarding these

estimates is that the unperturbed states are regarded as cubic and that trigonal crystal-field corrections are not needed to obtain nonzero K_E , but are necessary to obtain nonzero K_S . Put another way, nonzero K_E requires only the spin-orbit induced admixture of some orbital angular momentum into the orbital singlet ground state, which does not split the ground state and causes an isotropic shift of the ground-state g value from its spin-only value. Nonzero K_S requires also the trigonal-field admixtures which split the ground state and induce anisotropy in the g value. It is common⁹ to find K_S estimated as $\xi^2/\Delta E$, which is only correct for a basis with trigonal-field admixtures already included, and to find this estimate for K_S inappropriately compared to $K_E \sim (\xi/\Delta E)^2 J'$, leading to the erroneous conclusion that $K_E/K_S \sim J'/\Delta E \ll 1$. Such an estimate was employed in the original treatment of the Cr_2O_3 magnetic anisotropy¹⁰ and has been accepted uncritically by various workers, including the present author in I.¹¹

In assessing the possible origins of the magnetoelastic interaction it is important to note that the size of the contribution that a particular mechanism makes to the anisotropy may not be a reliable guide to the importance of the mechanism for the magnetoelastic interaction, since the latter involves the strain dependence of the mechanism. DES have concluded, from the rather small effect of hydrostatic pressure on the Néel temperature, that the strain dependence of the exchange interaction is too small to account for the variation with c -axis stress of the critical field for spin-flop. Hydrostatic pressure may produce strains with opposing effects and a better indication of the unimportance of the strain dependence of the exchange interaction is the slight sensitivity of the magnetic Davydov splittings in the optical spectrum to the application of uniaxial stress not exceeding the critical value for spin flop. DES² have also considered the contribution of the strain dependence of the dipole-dipole interaction to their magnetoelastic interaction parameters λ_1 and λ_2 , defined in Sec. II. They made use of the work of Artman, Murphy, and Foner,⁸ who calculated the effect on K_{MD} of strains preserving the crystal symmetry, and found that K_{MD} is quite sensitive not only to changes in the lattice parameters, but to the exact positions of the Cr^{3+} ions along the c axis. These positions are not completely determined by the corundum crystal structure symmetry, and the freedom is characterized by the metal-ion special position parameter w . Artman, Murphy, and Foner's work yields the following derivatives:

$$\frac{\partial K_{\text{MD}}}{\partial \epsilon_{zz}} = 1.36 \times 10^7 \text{ erg/cm}^3,$$

$$\frac{\partial K_{\text{MD}}}{\partial V} = -0.047 \times 10^7 \text{ erg/cm}^3, \quad (31)$$

$$\frac{\partial K_{\text{MD}}}{\partial \epsilon_w} = 0.65 \times 10^7 \text{ erg/cm}^3,$$

where $\epsilon_w \equiv \Delta w/w$ and $V \equiv \epsilon_{xx} + \epsilon_{yy} + \epsilon_{zz}$. These results can be used to find the contribution of the strain dependence of K_{MD} to the parameters λ'_1 and λ'_2 , defined in Sec. II. From their definitions and Eqs. (6), (7), and (8), it is readily shown that

$$\lambda'_1 = \frac{\partial K}{\partial \epsilon_{zz}} + \frac{\partial K}{\partial \epsilon_w} \frac{\partial \epsilon_w}{\partial \epsilon_{zz}}, \quad (32)$$

$$\lambda'_2 = \frac{\partial K}{\partial V} + \frac{\partial K}{\partial \epsilon_w} \frac{\partial \epsilon_w}{\partial V}.$$

These expressions are, of course, identical to the ones obtained by DES for their parameters λ_1 and λ_2 . As DES point out, the derivatives $\partial \epsilon_w/\partial \epsilon_{zz}$ and $\partial \epsilon_w/\partial V$ are not known. This is because the corundum structure has ions not at inversion centers, so that the actual ion movements accompanying a macroscopic strain cannot be computed. This is an important point that will arise again in the discussion below. Assuming that w does not change and combining Eqs. (31) and (32) gives

$$\lambda'_{1\text{MD}} = 1.36 \times 10^7 \text{ erg/cm}^3, \quad (33)$$

$$\lambda'_{2\text{MD}} = -0.47 \times 10^7 \text{ erg/cm}^3,$$

where the subscript MD implies the contribution is from the dipole-dipole interaction. The results in the second column of Table II can be deduced from the λ'_{MD} values and their definitions. Comparison with the experimental values shows that $\lambda'_{1\text{MD}}$ has a much smaller magnitude and a different sign from λ'_1 , while $\lambda'_{2\text{MD}}$ and λ'_2 agree quite well. DES point out that to improve the result for $\lambda'_{1\text{MD}}$ would require the assumption that $\partial \epsilon_w/\partial \epsilon_{zz} \approx -40$, which seems unlikely. They conclude that the strain dependence of the magnetic dipole interaction does not make a major contribution to the magnetoelastic interaction. This leaves unexplored the strain dependence of the single-ion anisotropy, which will be taken up next.

The single-ion anisotropy contribution to K , K_S , is given by¹⁰

$$K_S = -(0.198 \times 10^{-15})(S)(S - \frac{1}{2})(4N)(D) \text{ erg/cm}^3, \quad (34)$$

where N is the number of unit cells per cm^3 , $S = \frac{3}{2}$ for Cr^{3+} , and D is the coefficient, in cm^{-1} , of the single-ion spin-Hamiltonian term $-D(S_x^2 + S_y^2)$ or, equivalently, $+DS_z^2$. Similarly, the single-ion magnetoelastic contribution to F_{ij} , $F_{ij}(S)$, is given by

$$F_{ij}(S) = (0.198 \times 10^{-15})(S)(S - \frac{1}{2})(N) \sum_l G_{ji}(l) \text{ erg/cm}^3, \quad (35)$$

where $G_{ji}(l)$ in cm^{-1} is the magnetoelastic matrix

(Voigt notation) giving the strain-induced terms in the single-ion spin Hamiltonian for site l of a unit cell: $\sum_{ij} S_j G_{ji}(l) \epsilon_i$. The reversed indices on F_{ij} and G_{ji} merely reflect reversed row and column labels and are introduced here to make an easy connection to experimental data for the G_{ji} . There are four sites per unit cell, which accounts for the factor of 4 in Eq. (34). $G_{ji}(l)$ has the same non-zero elements as F_{ij} but in addition $G_{14} = -G_{24}$, $G_{15} = -G_{25} = -G_{64}$, $G_{16} = -G_{26} = -G_{61} = -G_{62}$, $G_{41} = -G_{42}$, $G_{51} = -G_{52} = -G_{46}$, and $G_{51} = -G_{54}$ are also nonzero.⁴ This form of $G_{ji}(l)$ is consistent with the C_3 site group symmetry of Cr_2O_3 . The effect of the elements not in C_3 but in the unitary subgroup D_3 of the magnetic factor group $D_{3d}(D_3)$ for Cr_2O_3 is to transform $G_{ji}(l)$ to $G_{ji}(l')$. It is found that the G_{ji} listed above change sign under these operations, while all other G_{ji} are unchanged, so that $\sum_l G_{ji}(l)$ has the same form as F_{ij} . Denoting by G_{ji} the matrix obtained by keeping only the elements of $G_{ji}(l)$ that are invariant, the expression for $F_{ij}(S)$ becomes

$$F_{ij}(S) = (0.198 \times 10^{-15})(S)(S - \frac{1}{2})(4N)G_{ji}. \quad (36)$$

The values of D and G_{ji} for the paramagnetic isomorph $\text{Al}_2\text{O}_3 : \text{Cr}^{3+}$ (ruby) have been experimentally determined by electron spin resonance in the absence and presence of uniaxial stress. D has been found¹² to be -0.19 cm^{-1} . Inserting this and $N = 1.04 \times 10^{22} \text{ cm}^{-3}$ in Eq. (34) gives $K_S = 23.5 \times 10^5 \text{ erg/cm}^3$. This is much larger than the number determined by Artman, Murphy, and Foner, which corresponds to a value of D of -0.0162 cm^{-1} (assuming $K_E = 0$). Thus, the ruby and Cr_2O_3 D values may be quite dissimilar. The application of the ruby G_{ij} to finding $F_{ij}(S)$ then entails the specific assumption that even though the D values may be different, the effect of strains in changing D and in inducing new lower symmetry terms into the spin Hamiltonian is nearly the same for ruby and Cr_2O_3 . That this may be a good assumption is suggested by the successful application of this kind of analysis to the magnetoelastic interactions of the rare-earth garnets¹³ and the iron-group monoxides¹⁴ by Phillips and White, whose work is the basis of this part of the discussion.

The experimental determination of G_{ji} for ruby has been carried out by Hemphill, Donoho, and McDonald.¹⁵ The form of the G matrix used by them is a special one that may be obtained from the F_{ij} and G_{ji} forms of this paper by the same procedure used in Sec. II to generate the altered F_{ij} of Eq. (6), namely, the subtraction from the strain-induced spin Hamiltonian of a term isotropic in the spin operators. In this case the subtracted term is

$$\left\{ \frac{1}{3}(G_{11} + G_{12} + G_{31})(\epsilon_{xx} + \epsilon_{yy}) \right.$$

$$\left. + \frac{1}{3}(G_{13} + G_{33})\epsilon_{zz} \right\} (S_x^2 + S_y^2 + S_z^2). \quad (37)$$

This leaves a spin Hamiltonian which has the same anisotropic properties as the original one and is generated by the following modified G_{ji} : $G_{11} - \frac{1}{3}(G_{11} - G_{12} - G_{31})$, $G_{12} - \frac{1}{3}(G_{12} - G_{11} - G_{31})$, $G_{13} = G_{23}$, $- \frac{1}{3}(G_{33} - G_{13})$, $G_{31} = G_{32} - \frac{1}{3}(G_{11} + G_{12} - 2G_{31})$, $G_{33} - \frac{2}{3}(G_{33} - G_{13})$. It is readily verified that the new G_{ji} satisfy the relations $G_{13} = G_{23} = -\frac{1}{2}G_{33}$ and $G_{31} = G_{32} = -(G_{11} + G_{12})$, present in the form of Hemphill, Donoho, and McDonald. The subtraction of an isotropic part from the interaction often reduces the number of independent elements in the interaction matrix (by two for the modified F_{ij} and G_{ji}) and never leads to any inconsistent results for physical quantities sensitive only to anisotropy.¹⁶ Thus it is no accident that the linear combinations of G_{ji} determined in the spin resonance experiments are exactly those needed to compute the linear combinations of F_{ij} appearing in the stress-induced spin-flop theory of Sec. II. Hemphill, Donoho, and McDonald give the following values, in cm^{-1} , for the modified G_{ji} : $G_{11} = 4.57$, $G_{12} = -1.94$, $G_{33} = 6.4$, $G_{44} = 1.97$, $G_{14} = -0.43$, $G_{41} = -0.63$. Substitution of these values in Eq. (36) and use of the above definitions of the modified G_{ji} then yield the numbers in the third column of Table II. Using these results and the approximate S_{ij} given in Sec. II, the theoretical contributions to α , β , γ and δ can be computed and these are given in the third column of Table III, along with the magnetic dipole contributions and the experimental numbers for the case $T_{1c} = -15 \text{ kbar}$, which are closer to the theoretical values than the numbers for the case $T_{1\beta} = -15 \text{ kbar}$. It should be noted that the entries in the first column and last two lines of Table II, and the last two columns of Table III depend on the S_{ij} , which are known only approximately.

Considering Tables II and III, it is convenient to discuss $(F_{31} - F_{33})$ and γ first. The experimental values of these quantities are probably the most reliable since γ and $\bar{\epsilon}_{zz}$, measured independently by DES, satisfy Eq. (15), and since $(F_{31} - F_{33})$ makes the major contribution to γ . The magnetic-dipole contribution to γ and $(F_{31} - F_{33})$ has the wrong sign and a magnitude much smaller than the experimental values, in contrast to the single-ion contribution, which has the correct sign and a magnitude roughly within a factor of 2 of the experimental values. Thus there appears to be a fairly consistent experimental and theoretical picture of the c -axis magnetoelastic behavior. Considering the remaining entries in the two tables, which concern primarily the basal-plane magnetoelastic behavior, the situation is not so clear. Lines seven and eight of Table II show fair sign and magnitude agreement between the single-ion and experimental results, but for $F_{11} + F_{12} - 2F_{13}$ the single-ion value

is of the wrong sign and has a much greater magnitude than the experimental number, while the magnetic dipole value agrees fairly well with the experimental one. Combining lines one and seven yields the last two lines of Table II. Assuming that F_{41} makes a small contribution to these quantities, as suggested by the single-ion results, the last two lines of Table II can be interpreted as showing particularly bad agreement between theory and experiment for $F_{11} - F_{13}$ and $F_{12} - F_{13}$ even though the difference of the two quantities shows fair agreement between theory and experiment (line seven of Table II). Using the experimental values for the case $T_{1\beta} = -15$ kbar yields even worse agreement.

Considering Table III, it is a curious fact that the $T_{1c} = -15$ kbar experimental values and the single-ion values for α and β are in fair agreement, in spite of the difficulties pointed out in Table II. These difficulties are reflected in the poorer agreement for $\alpha + \beta$. In view of the lack of S_{ij} values for Cr_2O_3 , and the incomplete determination of the experimental F_{ij} , it does not seem fruitful to speculate at length on the source of the disagreement in Tables II and III. One possibility deserves mention. The interpretation of the basal-plane magnetostriction data of DES rests on the assumption that the small basal-plane component of the applied magnetic field orients the spins in the basal plane. This assumption rests, in turn, on there being only a very small (fourth order in the spins) basal-plane anisotropy. However, if the basal-plane magnetoelastic interaction is strong and anisotropic, as suggested by the single-ion values of $(F_{11} - F_{13}) \pm (F_{12} - F_{13})$, then there may be a fairly large basal-plane anisotropy induced self-consistently by the magnetoelastic interaction. (Such an effect occurs in Fe_2O_3 , but the magnitude is small.^{17,18}) Thus it is possible that the measurements of DES have not yielded $\bar{\epsilon}(x)$, and that the experimental numbers of Table II are not correct, especially those involving F_{11} and F_{12} . This possibility can be investigated by further experiments.

IV. MICROSCOPIC THEORY OF SINGLE-ION EFFECTS

This section is a discussion of a more microscopic view of the single-ion anisotropy and magnetoelastic interaction. The discussion of the magnetoelastic interaction will be limited to considering the effect of stresses and strains that preserve the crystal symmetry, because for this case there is a large body of previous work upon which to draw, and because it is relevant to the parameter $F_{31} - F_{33}$, which is known with the least uncertainty. The discussion is largely a review and updating of what has been accomplished for the paramagnetic isomorph, ruby, but includes extensions to Cr_2O_3 wherever possible. Ideally such a program proceeds in two steps. In step one the $G_{ij}(l)$ are re-

TABLE III. Experimental and theoretical values of α , β , γ , and δ . The experimental values are for the case $T_{1c} = -15$ kbar of Table I.

	Experimental ($\times 10^5$)	Magnetic dipole ($\times 10^5$)	Single ion ($\times 10^5$)
α	1.33		3.07
β	-0.53		-0.33
$\alpha + \beta$	0.8		2.74
γ	-2.86	-0.27	-1.60
δ	mag. < 0.053	0.17	-0.22

lated to the strain dependence of the various lower-than-cubic symmetry components of the crystal field, and in step two the crystal field and its strain dependence are calculated from first principles. The work of a number of authors in the past ten years has been directed at various parts of this program for ruby.

Macfarlane¹⁹ has obtained the following approximate analytic expression for D in terms of the trigonal crystal-field parameters²⁰ v and v' , and the spin-orbit parameter ζ :

$$D = - (0.72 \times 10^{-8} \zeta^2 v' - 0.045 \times 10^{-8} \zeta^2 v). \quad (38)$$

He has shown that the values $v = 800 \text{ cm}^{-1}$, $v' = 680 \text{ cm}^{-1}$, and $\zeta = 180 \text{ cm}^{-1}$ yield a good over-all description of the spectroscopic data for ruby and, in particular, a value of $D = -0.147 \text{ cm}^{-1}$ is obtained from Eq. (38), as compared with the value -0.155 cm^{-1} obtained from numerical diagonalization of the single-ion Hamiltonian, and with the experimental value -0.19 cm^{-1} . Sturge²¹ has measured the changes induced by c -axis uniaxial stress in the first-order trigonal splittings of the ${}^2T_1(t_2^2)$ and ${}^2T_2(t_2^2)$ states, and in the second-order splitting of the ${}^2E(t_2^2)$ state of Cr^{3+} in ruby. These changes are denoted δ_1 , δ_2 , and δ_E , respectively. From his measurements, Sturge has deduced the stress-induced changes in v and v' , to be denoted v_s and v'_s , respectively, and then used these values to compute the effect of stress on the ground-state (4A_2) splitting $-2D$. The computed value is then compared to the experimental result obtained from the data of Hemphill, Donoho, and McDonald.¹⁵ It seems worthwhile to update his analysis, using the most recent numerical formulas of Macfarlane for the splitting changes induced by v_s and v'_s . The large first-order splittings of 2T_1 and 2T_2 are defined between the midpoint of the small spin-orbit-induced $2\bar{A} - \bar{E}$ splitting and the location of the second \bar{E} component of each state, where \bar{E} and $2\bar{A}$ label double-group representations of the site group C_3 . Macfarlane's numerical formulas are²²

$$\begin{aligned} \delta_E &= 0.027v_s + 0.008v'_s, \\ \delta_1 &= -0.036v_s + 0.315v'_s, \end{aligned} \quad (39)$$

$$\delta_2 = -0.2905v_s + 0.5225v'_s, \quad (39)$$

and Sturge's experimental results²¹ are

$$\delta_E = -0.057 \pm 0.004,$$

$$\delta_1 = 1.25 \pm 0.15,$$

$$\delta_2 = 3.5 \pm 0.3,$$

all in $\text{cm}^{-1}/\text{kbar}$ of compressive stress. A positive δ means an increase in the intrinsic ruby splittings. The values $(v_s, v'_s) = (-3.35, 4.2)$ in $\text{cm}^{-1}/\text{kbar}$ in Eq. (39) yield $\delta_E = -0.057$, $\delta_1 = 1.444$, and $\delta_2 = 3.168$, in $\text{cm}^{-1}/\text{kbar}$, nearly the experimental values for each. Macfarlane's numerical formula for the change in the ground-state splitting,²² denoted by δ_g is

$$\delta_g = -0.23 \times 10^{-4}v_s + 4.2 \times 10^{-4}v'_s, \quad (40)$$

and the above values of v_s and v'_s in Eq. (40) yield $\delta_g = 0.00184 \text{ cm}^{-1}/\text{kbar}$ of compressive stress. The data of Hemphill, Donoho, and McDonald yield the experimental value of δ_g according to the formula

$$\delta_g = -2\delta D = -\{2S_{13}(G'_{11} + G'_{12})(3) + 2S_{33}G'_{33}(-\frac{3}{2})\}(T_{zz}), \quad (41)$$

where the primed G_{ij} denote the definitions used by Hemphill, Donoho, and McDonald, discussed above. Setting $T_{zz} = -10^9 \text{ dyn}/\text{cm}^2$, using $S_{13} = -0.038 \times 10^{-13} \text{ cm}^2/\text{dyn}$, $S_{33} = 1.94 \times 10^{-13} \text{ cm}^2/\text{dyn}$, appropriate for Al_2O_3 ,²³ and using the experimental G'_{ij} in Eq. (41) yields the experimental $\delta_g = 0.00432 \text{ cm}^{-1}/\text{kbar}$ compressive stress. Thus the value from Eq. (40) has the same sign and a magnitude about 43% of the experimental value, somewhat less than the 60% reported by Sturge.²⁴ If v_s and v'_s are chosen by fitting the experimental data to the formulas for δ_E and δ_g , then the values -5.08 and $10.0 \text{ cm}^{-1}/\text{kbar}$ of compressive stress are found, respectively.²⁵ Despite the discrepancies, the agreement between the calculated and measured δ_g values is good enough to state that step one of the microscopic treatment has been carried through with reasonable success for ruby.

A similar treatment for Cr_2O_3 requires knowing v , v' , and their strain dependence in Cr_2O_3 (ξ may also change slightly from the ruby value). In principle, this information can be garnered from the optical spectrum, as was done for ruby, but in practice there is the difficulty of separating the effects of single-ion and interion interactions in the spectrum. McClure²⁶ has suggested that an approximate value of -700 cm^{-1} can be deduced for v from the splitting of the broad 4T_2 absorption band. An estimate for v' can be obtained by assuming that $K_E = 0$. Then $D = -0.00807 \text{ cm}^{-1}$ is deduced from Eq. (34) for $K_S = 10^5 \text{ erg}/\text{cm}^3$, and this small negative D can only be gotten from Eq. (38) by a cor-

respondingly small value of $v' = -9.16 \text{ cm}^{-1}$, assuming McClure's estimate of v . Changes in v can swing v' from small and negative to small and positive, but since v makes a small contribution to D , the basic conclusion is that $|v'|$ must be small if K_E is assumed to be zero. This point will be discussed further below. Accurately deducing the strain dependence of v and v' from the measurements of the effect of uniaxial stress on the optical spectrum does not appear possible at present because the S_{ij} are not known, because the strain dependence of the interion interactions are not known, and because the line broadening due to inhomogeneous applied stress makes small splitting changes difficult to determine. However, the reasonably good agreement for $F_{31} - F_{33}$ and γ between the experimental values and the single-ion ones deduced from ruby (see Tables II and III) suggests that the strain dependence of at least v' , and possibly v , may be similar in ruby and Cr_2O_3 even though the actual values of these parameters are probably different for the two materials.

In step two of a microscopic treatment, v , v' , and their strain dependence would be calculated from first principles, and some attempts at this have been made. Basically the calculations of v and v' are either based entirely on the point-charge model, or seek also to include the effects of covalent bonding and induced dipolar interactions. In ruby, assuming a Cr^{3+} ion occupies an Al^{3+} site, it is found that the point-charge model does badly for v , giving the wrong sign,²⁷ but that it gives v' with the right sign and the right order of magnitude.²⁴ It is an interesting empiric fact that the point-charge model frequently provides a reliable guide to the sign and magnitude of v' for various ions in Al_2O_3 ²⁴ and some other oxide lattices,²⁸ but is often wrong for v .²⁹ Point-charge formulas for v and v' in Cr_2O_3 can be obtained from McClure's calculations^{26,30} as

$$\begin{aligned} v &= -0.101\langle r^2 \rangle - 0.0267\langle r^4 \rangle \text{ eV}, \\ v' &= 0.0474\langle r^2 \rangle - 0.0098\langle r^4 \rangle \text{ eV}, \end{aligned} \quad (42)$$

where $\langle r^n \rangle$ has units of \AA^n . For the values of $\langle r^2 \rangle$ and $\langle r^4 \rangle$ there are three possibilities. The free-ion self-consistent-field (SCF) values³¹ can be used, or $\langle r^4 \rangle$ can be determined empirically by fitting a point-charge-model calculation of the cubic crystal-field parameter $10Dq$ to its experimental value and combined with the SCF value for $\langle r^2 \rangle$, or both $\langle r^4 \rangle$ and $\langle r^2 \rangle$ can be determined empirically by fitting the point-charge model with the experimental values for $10Dq$ and v . These three procedures yield, respectively, values²⁸ for $\langle r^2 \rangle$, $\langle r^4 \rangle$ in \AA^2 of (0.408, 0.341), (0.408, 3.0), and (0.065, 3.0), and values for (v, v') in cm^{-1} of (-407, 129), (-980, -85), and (-700, -212). Con-

sidering the general reliability of the point-charge estimate for v' , these results for v' are consistent with the conclusion obtained by assuming $K_E = 0$, that $|v'|$ may be near zero. However, from the arguments given at the outset of this section, K_S and K_E are expected to be comparable (in magnitude, but not necessarily in sign) if v' , which makes the major contribution to D , and J' are of comparable magnitude. The ground-state J values, which may indicate the order of magnitude of J' , are known³² to be $\approx 62 \text{ cm}^{-1}$ for the single nearest neighbor, and $\approx 27 \text{ cm}^{-1}$ for the three second-nearest neighbors, so the total K_E could well be comparable to K_S in Cr_2O_3 . The most that can be said at present is that although it does not appear to be necessary to set $K_E \neq 0$, this possibility cannot be excluded. It is interesting to note that the point charge value for v in Cr_2O_3 is also in fair accord with experiment. Although their results differ in detail, the work of McClure^{26,27} and of Artman and Murphy³³ has shown that the sign of v in ruby is sensitive to the exact position of the Cr^{3+} impurity along the c axis, which is not fixed by the corundum symmetry, and to possible local distortion of the lattice around the impurity. It is possible that the result for v in Cr_2O_3 is better because the ion positions are known accurately.

A rigorous point-charge calculation of v_s and v'_s for ruby or Cr_2O_3 is not possible because, as mentioned in discussing the strain dependence of K_{MD} , the corundum symmetry does not permit calculation of the actual ion movements that accompany a macroscopic strain. However, Kushida and Kikuchi³⁴ have suggested an approximate calculation of stress-induced effects for ruby based on point-charge calculations for various impurity ions in MgO. MgO is cubic until stressed and since every ion is at a site of inversion symmetry, the actual ion movements accompanying a stress can be deduced. It is a remarkable fact that the point-charge model with free-ion SCF values for the $\langle r^n \rangle$ applied to MgO: V^{2+} , Cr^{3+} gives values for v_s and v'_s in quite good agreement with experimental values.^{35,36,22} As usual, the model does not give the experimental $10Dq$ well at all.³⁵ Macfarlane²² gives the MgO formulas for v_s and v'_s as follows:

$$\begin{aligned} v_s &= 3\epsilon_{x'y'} \{1.704\langle r^2 \rangle / R^3 - 1.945\langle r^4 \rangle / R^5\}, \\ v'_s &= -3\epsilon_{x'y'} \{0.803\langle r^2 \rangle / R^3 + 0.687\langle r^4 \rangle / R^5\}. \end{aligned} \quad (43)$$

In these formulas R is the cubic lattice parameter and $\epsilon_{x'y'}$ is a shear strain with respect to the crystalline cubic axes. If R and $\langle r^n \rangle$ are in atomic units, then v_s and v'_s are in atomic units. Kushida and Kikuchi,³⁴ drawing upon the work of Blume *et al.*,³⁷ argue that because the oxygen octahedron surrounding a Cr^{3+} ion in ruby is only slightly distorted from cubic symmetry, the dominant stress-

induced shifts in crystal-field parameters can be calculated by employing the MgO formulas with R taken as the average separation between a Cr^{3+} ion and the six O^{2-} ions around it, this being³⁸ $R = 1.91 \text{ \AA} = 3.62 \text{ a.u.}$ For a trigonal strain, $\epsilon_{x'y'} = \epsilon_{y'z'}$ $= \epsilon_{z'x'}$, and it is straightforward to show³⁷ that

$$3\epsilon_{x'y'} = \{\epsilon_{zz} - \frac{1}{2}(\epsilon_{xx} + \epsilon_{yy})\} = (S_{33} - S_{13})T_{zz}, \quad (44)$$

where the unprimed coordinates are the ones used for Cr_2O_3 in this paper. Using the Cr^{3+} SCF values for $\langle r^2 \rangle$ and $\langle r^4 \rangle$ given previously, Eqs. (43) and (44) combine to give for (v_s, v'_s) the values $(-1.966, 1.502)$ in $\text{cm}^{-1}/\text{kbar}$ of compressive stress. These may be compared to the experimental values deduced from Eqs. (39), $(-3.35, 4.2)$, or the experimental values deduced from δ_E and δ_g , $(-5.08, 10.0)$. There is sign agreement between experiment and theory, but the magnitude agreement is not nearly so good as for MgO, especially since the experimental MgO values are deduced from δ_E and δ_g . Kushida and Kikuchi employed perturbation theory to calculate δ_E , δ_1 , and δ_2 from the point-charge model, and obtained very good agreement with Sturge's data. It is evident that if the point-charge-model v_s and v'_s obtained here are substituted in the numerical formulas of Macfarlane, Eq. (39), there will not be particularly good agreement with Sturge's data. The precise origin of this discrepancy is not immediately evident.³⁹

The assumption of cubic symmetry made in this analysis implies special relations among the G_{ij} . By combining Eqs. (40), (43), and (44), and comparing with Eq. (41), it is readily shown that

$$\frac{3}{2} G'_{33} = 3(G'_{11} + G'_{12}) = -\frac{1}{2}(ac + bc'), \quad (45)$$

where a and b are the coefficients of v_s and v'_s , respectively, in Eq. (40), and c and c' are the bracketed quantities in the expressions for v_s and v'_s , respectively, in Eq. (43). Inspecting the data of Hemphill, Donoho, and McDonald shows that the two G_{ij} quantities of Eq. (45) are indeed similar, but are about 5.5 times larger than the theoretical value. Thus the assumption of cubic symmetry is probably not, by itself, the principal flaw in the point-charge calculation. As mentioned above, the trigonal-field parameters in corundum are sensitive to small displacements of the metal-ion position and such effects are not included in this simple calculation. Also, the possible conceptual defects in the point-charge model itself cannot be dismissed.

The approximate point-charge calculation can also be applied directly to Cr_2O_3 . For Cr_2O_3 the average $R = 1.99 \text{ \AA} = 3.77 \text{ a.u.}$ ⁴⁰ The quantities a and b in Eq. (45) are best obtained from Eq. (38), since Eq. (40) is specific to ruby and centered about the ruby (v, v') values, which are not the same as in Cr_2O_3 . The quantities c and c' depend

on the choice of $\langle r^2 \rangle$ and $\langle r^4 \rangle$ values. By combining Eqs. (36) and (45), and using the previously stated interrelations between the primed (modified) G_{ji} and the unprimed G_{ji} , the following combinations of $F_{ij}(S)$ are deduced:

$$\begin{aligned} F_{11} + F_{12} - 2F_{13} &= 1.76 \times 10^7, 3.38 \times 10^7, \\ F_{31} - F_{33} &= -1.76 \times 10^7, -3.38 \times 10^7, \end{aligned} \quad (46)$$

all in erg/cm^3 . The left- and right-hand sets of values are obtained by using, respectively, the first and second sets of $\langle r^2 \rangle$ and $\langle r^4 \rangle$ given below Eq. (42). Equation (46) can be compared with Table II. As expected, the results have the same signs as the ones obtained from the ruby G_{ji} , but lower magnitudes. The effect of altering the $\langle r^4 \rangle$ value from the SCF to the empiric one is to make both v_s and v'_s positive for compressive stress and to increase the calculated F_{ij} quantities's magnitudes somewhat.

To summarize, the point-charge model with free-ion SCF values for the $\langle r^n \rangle$ works fairly well for v and v' in Cr_2O_3 where the ion positions are accurately known. The incorrect prediction of the sign of v in ruby may be due to uncertainty in the location of the metal ion. For both ruby and Cr_2O_3 an empiric value of $\langle r^4 \rangle$ that is much larger than the SCF one must be used to fit the experimental value of $10Dq$. The use of empiric values for $\langle r^2 \rangle$ and $\langle r^4 \rangle$ has a much smaller effect on the calculated values of v and v' . The point-charge model with SCF $\langle r^n \rangle$ values gives the experimentally observed signs for v_s and v'_s in ruby. If v_s and v'_s in Cr_2O_3 have the same signs as in ruby, there is also agreement for Cr_2O_3 . The prediction of opposite signs for v_s and v'_s hinges on the fact that for the SCF values, $(\langle r^2 \rangle / R^3) > (\langle r^4 \rangle / R^5)$. For Cr_2O_3 , and also for ruby, although the ruby calculation was not set forth explicitly above, the use of the larger, empiric $\langle r^4 \rangle$ value alters the sign of v_s . For ruby, the possibly for Cr_2O_3 , the altered sign is in disagreement with experiment. For MgO, where v and v' are zero, essentially the same observations can be made about $10Dq$, v_s , and v'_s . It seems to be a fair assessment to state that the point-charge model with free-ion SCF values for $\langle r^n \rangle$ is significantly more successful in calculating v , v' , v_s , and v'_s than $10Dq$. A final curious fact is that the variation of $10Dq$ with hydrostatic pressure generally has the $1/R^5$ dependence predicted by the point-charge model.

There have been some attempts to include the effects of covalent bonding and induced dipolar interactions⁴¹ in the theory of the trigonal crystal field of ruby. Stedman^{42,43} has constructed a phenomenological theory with essentially retains the form of the point charge model for the nearest-neighbor O^{2-} ions but generalizes the meaning of

the parameters. Contributions from O^{2-} ions other than the nearest neighbors are calculated on an ionic model, including monopolar and dipolar effects. The parameters of the model can be adjusted to fit the ruby $10Dq$, v , and v' values. Stedman⁴³ has also proposed a model for the local strains induced by c -axis stress and used his formulation to calculate v_s and v'_s in ruby. He obtains, in $\text{cm}^{-1}/\text{kbar}$ of compressive stress, $v_s = -4.7$ and $v'_s = 3.7$. These are in somewhat better agreement with the ruby experimental values than those of the approximate point-charge model given below Eq. (44). Although Stedman's theory is interesting, it does not provide insight into the role of covalency. Indeed, as Stedman points out, in its application to MgO the theory encounters an inconsistency between the calculation of $10Dq$ and of (v_s, v'_s) that is the counterpart of what happens for the point-charge model.

The most fundamental point of view for ruby was taken by Rimmer and Johnston,⁴⁴ who specifically calculated the covalent contributions to v and v' . Unfortunately, their calculation did not substantially improve on the point-charge-model results. It is also unfortunate that they did not calculate the cubic parameter $10Dq$, since it is in the theory of $10Dq$ that covalent effects have been shown most clearly to be of importance.

Feher and Sturge²⁴ have tried to assess, qualitatively, the relative importance of ionic and covalent contributions to v , v' , v_s , and v'_s in Al_2O_3 by examining these parameters for the isoelectronic sequence, V^{2+} , Cr^{3+} , Mn^{4+} , present diluted in Al_2O_3 . They compared the experimental variations of the parameters across the sequence to the variations predicted by McClure's point-charge-model formulas for v and v' for the case where the impurity ion occupies an Al^{3+} site. Due to the decrease in the SCF values for $\langle r^2 \rangle$ and $\langle r^4 \rangle$, the point-charge contributions decrease in magnitude with increasing nuclear charge. Since v' followed this trend, it was concluded that v' depends primarily on long-range electrostatic interactions, and not on covalent effects, which increase rapidly with increasing ionic charge. Although v does not follow the point-charge trend and increases its magnitude with increasing ionic charge, as does $10Dq$, Feher and Sturge were unwilling to attribute this to covalency effects, citing the success of the point-charge model for v_s and v'_s in MgO and arguing that the degree of covalency should be nearly the same for MgO and Al_2O_3 . They concluded only that v depends on short-range interactions and may be sensitive to the details of the local environment. Their argument against the importance of covalency for v does not seem very compelling. The experimental data for isoelectronic ions in MgO also do not follow the point-charge trends. In addition, it is not established that covalency has the same degree of

importance for v and v' as for v_s and v'_s . However, Feher and Sturge's analysis encounters the difficulty that the point-charge-model formulas themselves are somewhat uncertain for impurity ions in corundum, owing to their sensitivity to the exact location of the metal ion.^{26,27,33} Small differences in the positions of the isoelectronic ions might produce effects large enough to compete with the trends induced by the $\langle r^n \rangle$ and might provide an explanation for the increase in v with ionic charge. Thus Feher and Sturge's caution in not attributing large covalency effects to v may be justified. Stedman⁴³ has disputed the arguments and conclusions of Feher and Sturge more strongly. He argues that covalency is important for both v and v' and explains their opposite experimental trends with increasing nuclear charge as resulting from the increase, due to covalency, of the terms that are roughly analogous, in his theory, to the $\langle r^4 \rangle$ terms of the point-charge model. He states that these terms contribute with opposite signs to v and v' , thus producing the observed trends, but unfortunately, in both the point-charge-model expressions, and in Stedman's own expressions⁴⁵ for v and v' , these terms appear to occur with the same sign for both parameters. Thus the rather elegant approach of Feher and Sturge has not yielded the definite conclusions that might have been expected. In spite of the objections that can be made to their arguments, the possibility cannot be ignored that, for microscopic reasons not presently recognized, the importance of covalency may differ for different crystal-field parameters, even in the same crystal. For example, Kanamori⁴⁶ has argued that covalency is less important in calculating crystal field strengths of lower symmetry than it is for the cubic $10Dq$. Also, Zdansky⁴⁷ has calculated the covalency contributions to v_s and v'_s in MgO, and found them to be relatively small even though he scaled the covalency to fit its contribution to $10Dq$, which is relatively large. Thus there does appear

to be a trend, as noted above, for the point-charge model to be more successful for the trigonal than for the cubic crystal field.

V. SUMMARY AND CONCLUSIONS

In Sec. II a phenomenological analysis of the phenomena of uniaxial stress-induced spin flop in Cr_2O_3 was presented. The analysis is adequate to describe the observations in Cr_2O_3 and to reconcile the work of DES with the present work. The analysis also leads to a partial determination of the static magnetoelastic interaction constants in Cr_2O_3 . Section III discussed the origins of the magnetic anisotropy and magnetoelastic interaction in Cr_2O_3 . It was concluded that the magnetic anisotropy has contributions of nearly equal magnitude from single-ion anisotropy, the magnetic dipole-dipole interaction, and possibly the interion pseudodipolar interaction. The origin of the magnetoelastic interaction is somewhat unclear, although the strain dependence of the single-ion anisotropy of ruby is partially successful in explaining the Cr_2O_3 experimental results. Further experimental work will be required to resolve the various discrepancies discussed in Sec. III. In Sec. IV the microscopic theory of the single-ion anisotropy and magnetoelastic interaction in ruby and Cr_2O_3 was discussed. It was concluded that the Cr_2O_3 single-ion anisotropy deduced by setting the pseudodipolar contribution to zero is consistent with a microscopic theory, but that a nonzero pseudodipolar interaction cannot be excluded. It was also concluded that the point-charge model for the trigonal crystal field and its strain dependence is significantly more successful than when applied to calculating the cubic field.

ACKNOWLEDGMENTS

It is a pleasure to acknowledge a number of valuable discussions with M. D. Sturge, R. M. Macfarlane, J. B. Goodenough, and H. J. Zeiger.

[†]Work sponsored by the Department of the U.S. Air Force.

¹J. W. Allen, Phys. Rev. Lett. **27**, 1526 (1971).

²K. L. Dudko, V. V. Eremenko, and L. M. Semenenko, Phys. Status Solidi **43**, 471 (1971).

³For similar treatments of other magnetoelastic phenomena see, e.g., A. I. Mitsek, Fiz. Met. Metalloved. **16**, 168 (1963); A. S. Pakhomov, Fiz. Met. Metalloved. **25**, 769 (1968).

⁴W. P. Mason, *Physical Acoustics and the Properties of Solids* (Van Nostrand, Princeton, N.J., 1958). Note that for Mason's matrices, one index j labels quantities defined without the customary Voigt notation factor of 2 for $j=4, 5$, and 6. Note also that the corundum factor group, rather than site group symmetry has been assumed, limiting F_{ij} to be a static interaction matrix. To describe dynamic effects like spin-phonon coupling a site magnetoelastic interaction must be used [see the discussion below Eq. (35), and the work of M. Boiteux *et al.*, [Phys. Rev. B **4**, 3077 (1971)] determining two Cr_2O_3 site interactions}.

⁵K. L. Dudko, V. V. Eremenko, and L. M. Semenenko, Phys. Lett. A **30**, 459 (1969).

⁶G. K. Lewis and H. G. Drickamer, J. Chem. Phys. **45**, 224 (1966).

⁷J. H. Gieske and Y. R. Barsch, Phys. Status Solidi **29**, 121 (1968).

⁸J. O. Artman, J. C. Murphy, and S. Foner, Phys. Rev. **138**, A912 (1965).

⁹See, for example, T. Moriya, in *Magnetism*, edited by G. T. Rado and H. Suhl (Academic, New York, 1963), Vol. 1.

¹⁰M. Tachiki and T. Nagamiya, J. Phys. Soc. Jap. **13**, 452 (1958).

¹¹The author is indebted to M. D. Sturge for these observations.

¹²A. A. Manenkov and A. M. Prokhorov, Zh. Eksp. Teor. Fiz. **28**, 762 (1955) [Sov. Phys.-JETP **1**, 611 (1955)].

¹³T. G. Phillips and R. L. White, Phys. Rev. Lett. **16**, 650 (1966).

- ¹⁴T. G. Phillips and R. L. White, *Phys. Rev.* **153**, 616 (1967).
- ¹⁵R. B. Hemphill, P. L. Donoho, and E. D. McDonald, *Phys. Rev.* **146**, 329 (1966).
- ¹⁶R. J. Harrison and P. L. Sagalyn, *Phys. Rev.* **128**, 1630 (1962).
- ¹⁷S. Iida and A. Tasaki, in *Proceedings of the International Conference on Magnetism, Nottingham, 1964* (The Institute of Physics and the Physical Society, London, 1964), p. 583.
- ¹⁸E. A. Turov and V. G. Shavrov, *Sov. Phys.-Solid State* **7**, 166 (1965).
- ¹⁹R. M. Macfarlane, *J. Chem. Phys.* **47**, 2066 (1967).
- ²⁰The one-electron trigonal field parameters ν and ν' are defined by M. H. L. Pryce and W. A. Runciman, *Discuss. Faraday Soc.* **26**, 34 (1958). Qualitatively, note that ν is a matrix element within the cubic t manifold, and that ν' is a matrix element between the cubic t and e manifolds.
- ²¹M. D. Sturge, *J. Chem. Phys.* **43**, 1826 (1965).
- ²²R. M. Macfarlane, *Phys. Rev.* **158**, 252 (1966); and private communication. The splitting formulas result from a numerical diagonalization of the crystal-field Hamiltonian with zero-stress parameters, and a first-order perturbation theory about the zero-stress parameters.
- ²³H. B. Huntington, *Solid State Physics*, edited by F. Seitz and D. Turnbull (Academic, New York, 1956), Vol. 7. These values differ slightly, but unimportantly from those of Ref. 7.
- ²⁴E. Feher and M. D. Sturge, *Phys. Rev.* **172**, 244 (1968). See footnote 10 of this reference.
- ²⁵The value for ν'_s given in Table III of Ref. 22 is incorrect by about a factor of 2 owing to the use of $-D$ rather than $-2D$ for δ_g in Table II of Ref. 22.
- ²⁶D. S. McClure, *J. Chem. Phys.* **38**, 2289 (1963).
- ²⁷D. S. McClure, *J. Chem. Phys.* **36**, 2757 (1962).
- ²⁸See, for example, M. D. Sturge, F. R. Merritt, J. C. Hensel, and J. P. Remeika, *Phys. Rev.* **180**, 402 (1969).
- ²⁹M. D. Sturge (private communication).
- ³⁰The Cr_2O_3 formula for ν' given in Table II of Ref. 26 is incorrect. The formula in the text, Eq. (42), is obtained by combining the potential constants of Table I of Ref. 26 with Eqs. (5) and (6) of Ref. 27, a procedure that yields the other formulas given in Table II of Ref. 26.
- ³¹R. E. Watson, Tech. Report No. 12, Solid State and Molecular Theory Group, MIT, Cambridge, Mass. (unpublished); and footnote 6 of Ref. 27.
- ³²E. J. Samuelsen, M. T. Hutchings, and G. Shirane, *Physica* **48**, 13 (1970).
- ³³J. O. Artman and J. C. Murphy, *Phys. Rev.* **135**, A1622 (1964).
- ³⁴T. Kushida and M. Kikuchi, *J. Phys. Soc. Jap.* **23**, 1333 (1967).
- ³⁵A. L. Schawlow, A. H. Piksis, and S. Sugano, *Phys. Rev.* **122**, 1469 (1961).
- ³⁶M. D. Sturge, *Phys. Rev.* **131**, 1456 (1963).
- ³⁷M. Blume, R. Orbach, A. Kiel, and S. Geschwind, *Phys. Rev.* **139**, A314 (1965).
- ³⁸R. W. G. Wyckoff, *Crystal Structures* (Interscience, New York, 1951).
- ³⁹If the various formulas of Ref. 34 are written in terms of ν_s and ν'_s , rather than the parameters Y and Z used there, it is found that ν_s and ν'_s are a factor of 2 larger than obtained here, and that the formulas for δ_E, δ_1 , and δ_2 are similar to those of Eq. (39) except in the δ_E coefficient of ν'_s and the δ_1 coefficient of ν_s . The latter differences might be expected to occur between results obtained from perturbation theory and numerical diagonalization.
- ⁴⁰R. E. Newnham and Y. M. DeHaan, *Z. Kristallogr.* **117**, 235 (1962).
- ⁴¹R. R. Sharma and T. P. Das, *J. Chem. Phys.* **41**, 3581 (1964).
- ⁴²G. E. Stedman, *J. Chem. Phys.* **50**, 1461 (1969).
- ⁴³G. E. Stedman, *J. Chem. Phys.* **51**, 4123 (1969).
- ⁴⁴D. E. Rimmer and D. F. Johnston, *Proc. Phys. Soc. Lond.* **89**, 953 (1966).
- ⁴⁵See Eq. (5) of Ref. 42.
- ⁴⁶J. Kanamori, *Prog. Theor. Phys. Suppl.* **17**, 197 (1956).
- ⁴⁷K. Zdankys, *Phys. Rev.* **159**, 201 (1967).

Impurity Excitations in Induced-Moment Systems in the Paramagnetic Phase; Some Effects of Additional Exchange Coupling*

Eugene Shiles

Department of Physics, Virginia Commonwealth University, Richmond, Virginia 23220

(Received 18 December 1972)

The impurity excitations characteristic of a single impurity in a paramagnetic induced-moment crystal are examined in a model that includes second-neighbor exchange coupling. All ions are assumed to have a singlet crystal-field ground state and singlet lowest excited state. Earlier calculations assuming only nearest-neighbor exchange found only s -type impurity modes in this type of system. It is found that the more complex exchange coupling may introduce additional s -type modes, and under certain conditions modes of other symmetry may appear. The qualitative results are valid for a general lattice.

I. INTRODUCTION

Recently, Wang and Cooper¹ discussed, using Green's-function theory and a pseudospin formalism, the collective excitations that may be characteristic of pure induced-moment crystals. For the crystals in the paramagnetic phase, these excitations are

magnetic excitons. More recently, several papers^{2,3} examined the changes in the magnetic excitation spectrum when substitutional impurities are placed in a paramagnetic induced-moment system. The problem has also been discussed for the system in the ordered phase.⁴ In Ref. 3, hereafter called I, it was found that only s -type impurity